Local Projection Stabilisation on Layer-Adapted Meshes for Convection-Diffusion Problems with Characteristic Layers (Part I and II)

Sebastian Franz and Gunar Matthies

Abstract For a singularly perturbed convection-diffusion problem with exponential and characteristic boundary layers on the unit square a discretisation based on layer-adapted meshes is considered. The standard Galerkin method and the local projection scheme are analysed for a general class of higher order finite elements based on local polynomial spaces lying between $\mathcal{P}_p$ and $\mathcal{Q}_p$. We will present two different interpolation operators for these spaces. The first one is based on values at vertices, weighted edge integrals and weighted cell integrals while the second one is based on point values only. The influence of the point distribution on the errors will be studied numerically.

We show convergence of order p in the ε-weighted energy norm for both the Galerkin method and the local projection scheme. Furthermore, the local projection methods provides a supercloseness result of order p in local projection norm.

1 Introduction

Let the singularly perturbed convection-diffusion problem be given by

$$-\varepsilon\Delta u - bu_x + cu = f \qquad \text{in } \Omega = (0,1)^2, \tag{1a}$$

$$u = 0 \qquad \text{on } \Gamma = \partial\Omega \tag{1b}$$

under the assumption that $b \in W^1_\infty(\Omega), c \in L_\infty(\Omega), b \geq \beta > 0$ with some constant β, and a small perturbation parameter $0 < \varepsilon \ll 1$.

S. Franz (✉)
Department of Mathematics and Statistics, University of Limerick, Limerick, Ireland
e-mail: sebastian.franz@ul.ie

G. Matthies
Universität Kassel, Fachbereich 10, Institut für Mathematik, Heinrich-Plett-Straße 40, 34132 Kassel, Germany
e-mail: matthies@mathematik.uni-kassel.de

C. Clavero et al. (eds.), *BAIL 2010 – Boundary and Interior Layers, Computational and Asymptotic Methods*, Lecture Notes in Computational Science and Engineering 81,
DOI 10.1007/978-3-642-19665-2_14,

This combination gives rise to an exponential layer of width $\mathcal{O}(\varepsilon)$ near the outflow boundary at $x = 0$ and to two parabolic layers of width $\mathcal{O}\left(\sqrt{\varepsilon}\right)$ near the characteristic boundaries at $y = 0$ and $y = 1$.

Problem (1) possesses a unique solution in $H_0^1(\Omega) \cap H^2(\Omega)$ if

$$c + b_x/2 \geq \gamma > 0 \tag{2}$$

holds. Assumption (2) can always be guaranteed by a simple transformation $\tilde{u}(x, y) = u(x, y)\mathrm{e}^{\varkappa x}$ with a suitably chosen constant $\varkappa$.

Due to the layers standard discretisations will not give accurate approximations on quasi-uniform meshes except the mesh width is of the same order as ε. Thus layer-adapted meshes based on *a priori* knowledge of the solution behaviour have been constructed, see [2, 18, 20]. We will use so called S-type meshes [19] combining the transition point of a standard Shishkin mesh and mesh generating functions inside the fine part.

Since the standard Galerkin methods lacks stability even on layer-adapted meshes, see [15, 21], a stabilisation term will be added to the standard discretisation. We will consider the one-level approach of the local projection stabilisation (LPSFEM), [3–5, 17]. However, we will not use enriched $\mathcal{Q}_r$-elements but consider a general class of higher order elements. To this end, let $p \geq 2$ be an arbitrary but fixed integer to indicate the polynomial degree of our ansatz functions.

This paper contains a condensed analysis of the LPSFEM applied to (1) on S-type meshes. For a full analysis see [11, 12].

Notation. In this paper, C denotes a generic constant which is always independent of the diffusion coefficient ε and the mesh parameter N. The usual Sobolev spaces $W_r^m(D)$ and $L_r(D)$ on any measurable two-dimensional subset $D \subset \Omega$ are used. We write $H^m(D)$ instead of $W_2^m(D)$ in the case $r = 2$. The $L_2(D)$-norm is denoted by $\|\cdot\|_{0,D}$ while the $(\cdot,\cdot)_D$ is the $L_2(D)$-inner product. The subscript D will always be dropped if $D = \Omega$.

By $\mathcal{P}_r(D)$ we denote the space of all polynomials with total degree less than or equal to r while $\mathcal{Q}_r(D)$ is the space of all polynomials with degree less than or equal to r in each variable separately.

2 Solution Decomposition and Layer-Adapted Meshes

We suppose there exists the following decomposition of the solution u of (1).

Assumption 1. The solution u of (1) can be decomposed as

$$u = v + w_1 + w_2 + w_{12}$$

where we have for all $x, y \in [0, 1]$ and $0 \leq i + j \leq p + 1$ the pointwise estimates

$$\left|\frac{\partial^{i+j} v}{\partial x^i \partial y^j}(x,y)\right| \le C, \quad \left|\frac{\partial^{i+j} w_1}{\partial x^i \partial y^j}(x,y)\right| \le C\varepsilon^{-i} \mathrm{e}^{-\beta x/\varepsilon},$$

$$\left|\frac{\partial^{i+j} w_2}{\partial x^i \partial y^j}(x,y)\right| \le C\varepsilon^{-j/2} \left(\mathrm{e}^{-y/\sqrt{\varepsilon}} + \mathrm{e}^{-(1-y)/\sqrt{\varepsilon}}\right),$$

$$\left|\frac{\partial^{i+j} w_{12}}{\partial x^i \partial y^j}(x,y)\right| \le C\varepsilon^{-(i+j/2)} \mathrm{e}^{-\beta x/\varepsilon} \left(\mathrm{e}^{-y/\sqrt{\varepsilon}} + \mathrm{e}^{-(1-y)/\sqrt{\varepsilon}}\right),$$

where w_1 covers the exponential boundary layer, w_2 the parabolic boundary layers, w_{12} the corner layers, and v is the regular part.

Remark 2. Kellogg and Stynes [14] proved the validity of Assumption 1 in the case of constant functions b, c provided f is smooth enough and fulfils certain compatibility conditions.

When discretising (1), we use in both x- and y-direction *S-type meshes* with N mesh intervals each. For this purpose let the mesh transition parameters be

$$\lambda_x := \frac{\sigma\varepsilon}{\beta} \ln N \le \frac{1}{2} \quad \text{and} \quad \lambda_y := \sigma\sqrt{\varepsilon} \ln N \le \frac{1}{4}$$

with some user-chosen positive parameter $\sigma \ge p+1$, where we assume for the mere sake of simplicity

$$\varepsilon \le \min\left\{\frac{\beta}{2\sigma}(\ln N)^{-1}, \frac{1}{16\sigma^2}(\ln N)^{-2}\right\}.$$

In the following, we assume that N is a multiple of 4. The domain Ω will be dissected by a tensor product mesh according to

$$x_i := \begin{cases} \frac{\sigma\varepsilon}{\beta}\phi\left(\frac{i}{N}\right), & i = 0, \ldots, N/2, \\ 1 - 2(1-\lambda_x)(1-\frac{i}{N}), & i = N/2, \ldots, N, \end{cases}$$

and

$$y_j := \begin{cases} \sigma\sqrt{\varepsilon}\phi\left(\frac{2j}{N}\right), & j = 0, \ldots, N/4, \\ (1-2\lambda_y)(\frac{2j}{N}-1) + \frac{1}{2}, & j = N/4, \ldots, 3N/4, \\ 1 - \sigma\sqrt{\varepsilon}\phi\left(2 - \frac{2j}{N}\right), & j = 3N/4, \ldots, N, \end{cases}$$

where ϕ is a monotonically increasing mesh-generating function satisfying $\phi(0) = 0$ and $\phi(1/2) = \ln N$. Given an arbitrary function ϕ fulfilling these conditions, an S-type mesh is defined. The final mesh is constructed by drawing lines parallel to the coordinate axes through these mesh points and is denoted by T^N. Figure 1 shows two examples of such meshes. The domain Ω is divided into the subdomains

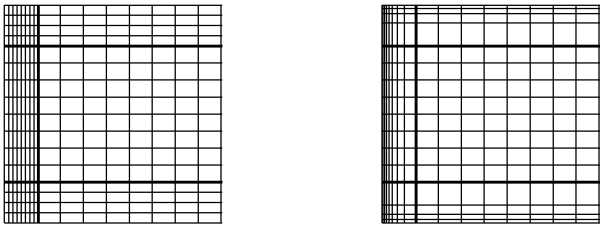

Fig. 1 Two S-type meshes: Shishkin mesh (*left*), Bakhvalov-Shishkin mesh (*right*)

with $\Omega_{12} := [0, \lambda_x] \times [\lambda_y, 1-\lambda_y]$ covering the exponential layer, $\Omega_{21} := [\lambda_x, 1] \times \big([0, \lambda_y] \cup [1-\lambda_y, 1]\big)$ the parabolic layers, $\Omega_{22} := [0, \lambda_x] \times \big([0, \lambda_y] \cup [1-\lambda_y, 1]\big)$ the corner layers, and $\Omega_{11} := [\lambda_x, 1] \times [\lambda_y, 1-\lambda_y]$ the remaining non-layer region.

Related to the mesh-generating function ϕ, we define by $\psi = \mathrm{e}^{-\phi}$ the mesh-characterising function ψ whose derivative yields information on the approximation quality of the mesh.

Two representatives of those meshes are the original Shishkin mesh [18] with $\phi(t) = 2t \ln N$ and $\max |\psi'| = 2 \ln N$, and the Bakhvalov-Shishkin mesh [16] with $\phi(t) = -\ln(1 - 2t(1 - N^{-1}))$ and $\max |\psi'| = 2$. Both meshes are shown in Fig. 1.

We assume for simplicity of the presentation that the maximal mesh sizes inside the layer regions

$$h := \max_{i=1,\dots,N/2} x_i - x_{i-1} \quad \text{and} \quad k := \max_{j=1,\dots,N/4} y_j - y_{j-1}$$

are both smaller than $CN^{-1} \max |\psi'|$.

3 General Finite Element Spaces and Interpolation

Let us come to the definition of the general local finite element space. It is given by

$$\mathcal{Q}_p^{\clubsuit}(\hat{\tau}) = \operatorname{span}\Big\{ \{1, \xi\} \times \{1, \eta, \dots, \eta^p\} \cup \{1, \xi, \dots, \xi^p\} \times \{1, \eta\} \cup \xi^2 \eta^2 \widetilde{\mathcal{Q}}(\hat{\tau}) \Big\}$$

with the space

$$\widetilde{Q}(\hat{\tau}) := \operatorname{span}\big\{ \xi^i \eta^j \ : \ i = 0, \dots, p-2, \ j = 0, \dots, k_i \big\}$$

satisfying $\mathcal{P}_{p-4}(\hat{\tau}) \subset \widetilde{\mathcal{Q}}(\hat{\tau}) \subset \mathcal{Q}_{p-2}(\hat{\tau})$ and $k_i \geq k_{i+1}$ for $i = 0, \dots, p-3$. Figure 2 shows a graphical representation of two example of $\mathcal{Q}_p^{\clubsuit}(\hat{\tau})$ in the case $p = 9$. A square at position (i, j) represents a basis function $\xi^i \eta^j$ of $\mathcal{Q}_p^{\clubsuit}(\hat{\tau})$. The

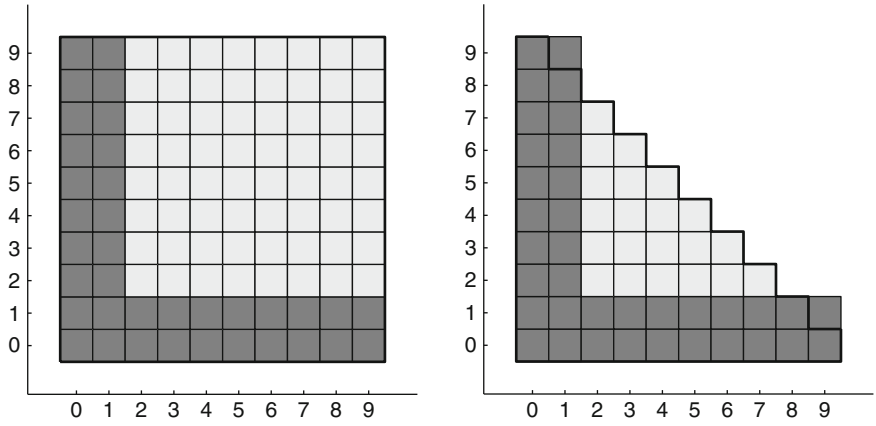

Fig. 2 Full space $\mathcal{Q}_p(\hat{\tau})$ (*left*), Serendipity space $\mathcal{Q}_p^{\oplus}(\hat{\tau})$ (*right*)

darker squares correspond to those functions present in all spaces we consider, while the lighter ones represent $\xi^2\eta^2\widetilde{\mathcal{Q}}(\hat{\tau})$. The left picture of Fig. 2 shows the standard $\mathcal{Q}_p$-space governed by taking $\widetilde{\mathcal{Q}}(\hat{\tau}) = \mathcal{Q}_{p-2}(\hat{\tau})$, while the right picture presents the serendipity space $\mathcal{Q}_p^{\oplus}$ defined by $\widetilde{\mathcal{Q}}(\hat{\tau}) = \mathcal{P}_{p-4}(\hat{\tau})$ for $p \geq 4$ and $\widetilde{\mathcal{Q}}(\hat{\tau}) = \emptyset$ for $p = 2, 3$.

We define our global finite element space as

$$V^N := \left\{ v \in H_0^1(\Omega) : v|_\tau \in \mathcal{Q}_p^{\clubsuit}(\tau) \ \forall \tau \in T^N \right\}$$

where $\mathcal{Q}_p^{\clubsuit}(\tau)$ is obtained from $\mathcal{Q}_p^{\clubsuit}(\hat{\tau})$ in the usual way by using the reference mapping $F_\tau : \hat{\tau} \to \tau$.

We now define two different interpolation operators. First, we consider an interpolation operator based on point evaluation at the vertices, line integrals along the edges and integrals over the cell interior.

Let $\hat{a}_i$ and $\hat{e}_i$, $i = 1, \ldots, 4$, denote the vertices and edges of the reference element $\hat{\tau}$, respectively. We define the vertex-edge-cell interpolation operator $\mathcal{I} : C(\hat{\tau}) \to \mathcal{Q}_p^{\clubsuit}(\hat{\tau})$ by

$$\mathcal{I}\hat{v}(\hat{a}_i) = \hat{v}(\hat{a}_i), \quad i = 1, \ldots, 4, \tag{3a}$$

$$\int_{\hat{e}_i} (\mathcal{I}\hat{v})\hat{q} = \int_{\hat{e}_i} \hat{v}\hat{q}, \quad i = 1, \ldots, 4, \quad \hat{q} \in \mathcal{P}_{p-2}(\hat{e}_i), \tag{3b}$$

$$\iint_{\hat{\tau}} (\mathcal{I}\hat{v})\hat{q} = \iint_{\hat{\tau}} \hat{v}\hat{q}, \qquad \hat{q} \in \widetilde{\mathcal{Q}}(\hat{\tau}). \tag{3c}$$

It can be proved that this interpolation operator is uniquely defined.

The interpolation operator $\mathcal{I}$ on the reference element $\hat{\tau}$ induces the global interpolation operator $I^N : C(\overline{\Omega}) \to V^N$ by

$$(I^N v)|_\tau := F_\tau \circ \mathcal{I} \circ F_\tau^{-1}(v|_\tau) \quad \forall \tau \in T^N,\ v \in C(\overline{\Omega}), \tag{4}$$

with the bijective reference mapping $F_\tau : \hat{\tau} \to \tau$.

Theorem 3. *For the finite element space V^N and the vertex-edge-cell interpolation operator I^N defined by (3) and (4), there holds the L_∞-stability*

$$\left\| I^N w \right\|_{L_\infty(\tau)} \leq C \|w\|_{L_\infty(\tau)} \quad \forall w \in C(\tau),\ \forall \tau \subset \overline{\Omega},$$

and the anisotropic error estimates

$$\begin{aligned}
\left\| w - I^N w \right\|_{L_q(\tau_{ij})} &\leq C \sum_{r=0}^{s} \left\| h_i^{s-r} k_j^r \frac{\partial^s w}{\partial x^{s-r} \partial y^r} \right\|_{L_q(\tau_{ij})}, \\
\left\| (w - I^N w)_x \right\|_{L_q(\tau_{ij})} &\leq C \sum_{r=0}^{t} \left\| h_i^{t-r} k_j^r \frac{\partial^{t+1} w}{\partial x^{t-r+1} \partial y^r} \right\|_{L_q(\tau_{ij})}, \\
\left\| (w - I^N w)_y \right\|_{L_q(\tau_{ij})} &\leq C \sum_{r=0}^{t} \left\| h_i^{t-r} k_j^r \frac{\partial^{t+1} w}{\partial x^{t-r} \partial y^{r+1}} \right\|_{L_q(\tau_{ij})}
\end{aligned}$$

for $\tau_{ij} \subset \overline{\Omega}$ and $q \in [1, \infty]$, $2 \leq s \leq p+1$, $1 \leq t \leq p$.

Using the technique given in [1] this theorem can be proved. Details can be found in [11].

The second interpolation operator we are interested in, is a point-value oriented interpolation operator. We consider two increasing sequences of $p+1$ points $-1 = \xi_0 < \xi_1 < \cdots < \xi_{p-1} < \xi_p = +1$ and $-1 = \eta_0 < \eta_1 < \cdots < \eta_{p-1} < \eta_p = +1$. The point-value oriented interpolation operator $\mathcal{J} : C(\hat{\tau}) \to \mathcal{Q}_p^{\clubsuit}(\hat{\tau})$ is defined by values on the edges including the vertices

$$(\mathcal{J}\hat{v})(\xi_i, \pm 1) := \hat{v}(\xi_i, \pm 1), \qquad i = 0, \ldots, p, \tag{5a}$$

$$(\mathcal{J}\hat{v})(\pm 1, \eta_j) := \hat{v}(\pm 1, \eta_j), \qquad j = 1, \ldots, p-1, \tag{5b}$$

and values in the interior

$$(\mathcal{J}\hat{v})(\xi_{i+1}, \eta_{j+1}) := \hat{v}(\xi_{i+1}, \eta_{j+1}), \qquad i = 0, \ldots, p-2,\ j = 0, \ldots, k_i. \tag{5c}$$

The interpolation operator $\mathcal{J}$ is uniquely determined, see [11] for details. Similarly as before we can define a global interpolation operator $J^N : C(\overline{\Omega}) \to V^N$ using the bijective reference mapping F_τ. It can be shown that all results from Theorem 3 are also valid for J^N. For details we refer again to [11].

4 Numerical Method and Convergence

We derive in this section bounds on the interpolation error and prove convergence of the Galerkin method and the LPSFEM. Although we will give in this section only results for the interpolation operator I^N, the same results hold true for the operator J^N. With the usual Galerkin bilinear form

$$a_{Gal}(u,v) := \varepsilon(\nabla u, \nabla v) + (cu - bu_x, v), \qquad u, v \in H_0^1(\Omega),$$

associated with problem (1), the standard Galerkin formulation of (1) is given by:

Find $\tilde{u}^N \in V^N$ such that

$$a_{Gal}(\tilde{u}^N, v^N) = (f, v^N) \qquad \forall v^N \in V^N. \tag{6}$$

Since the standard Galerkin discretisation lacks stability even on S-type meshes [15, 21], the local projection method is applied for stabilisation. Let π_τ denote the L_2-projection into the finite dimensional function space $D(\tau) := \mathcal{P}_{p-2}(\tau)$. The fluctuation operator $\kappa_\tau : L_2(\tau) \to L_2(\tau)$ is defined by $\kappa_\tau v := v - \pi_\tau v$.

In order to get additional control on the derivative in streamline direction, we define the stabilisation term

$$s(u,v) := \sum_{\tau \in T^N} \delta_\tau \big(\kappa_\tau(bu_x), \kappa_\tau(bv_x)\big)_\tau$$

with the cell-dependent parameters $\delta_\tau \geq 0$, $\tau \in T^N$, which will be constant inside each subdomain of Ω, i.e., $\delta_\tau = \delta_{ij}$ for $\tau \subset \Omega_{ij}$. It was stated in [10] for different stabilisation methods that stabilisation is best if only applied in $\Omega_{11} \cup \Omega_{21}$. Therefore, we set $\delta_{12} = \delta_{22} = 0$ in the following.

The stabilised discrete problem reads:

Find $u^N \in V^N$ such that

$$a_{LPS}(u^N, v^N) := a_{Gal}(u^N, v^N) + s(u^N, v^N) = (f, v^N) \qquad \forall v^N \in V^N. \tag{7}$$

The subsequent analysis uses the ε-weighted energy- and the LPS-norm

$$|||v|||_\varepsilon := \left(\varepsilon \|\nabla v\|_0^2 + \gamma \|v\|_0^2\right)^{1/2} \quad \text{and} \quad |||v|||_{LPS} := \left(|||v|||_\varepsilon^2 + s(v,v)\right)^{1/2}.$$

Theorem 4 (Interpolation error). *Let the solution u of (1) fulfil Assumption 1. Then, the interpolation operator I^N provides the following pointwise interpolation error bounds*

$$\left\| I^N u - u \right\|_{L_\infty(\Omega_{11})} \leq C N^{-(p+1)},$$
$$\left\| I^N u - u \right\|_{L_\infty(\Omega \setminus \Omega_{11})} \leq C \left(N^{-1} \max |\psi'| \right)^{p+1}.$$

Moreover, the L_2- and energy norm bounds

$$\left\| I^N u - u \right\|_0 \leq C \left(N^{-1} \max |\psi'| \right)^{p+1} \text{ and } \left| \left| \left| I^N u - u \right| \right| \right|_\varepsilon \leq C \left(N^{-1} \max |\psi'| \right)^p$$

hold true.

The proof of Theorem 4 uses the decomposition of Assumption 1 and Theorem 3 to bound the different parts of u in the several subdomains of Ω. Note the appearance of $\max |\psi'|$ in the estimates that refers to the quality of the underlying mesh.

Theorem 5 (Convergence Galerkin FEM and LPSFEM). *Let the solution u of (1) satisfy Assumption 1 and let $\tilde{u}^N$ denote the Galerkin solution of (6). We set*

$$C_\psi := 1 + N^{-1/2} \ln^{1/2} N \max |\psi'|. \tag{8}$$

Then, we have

$$\left| \left| \left| u - \tilde{u}^N \right| \right| \right|_\varepsilon \leq C C_\psi \left(N^{-1} \max |\psi'| \right)^p.$$

Let the LPSFEM solutions of (7) be denoted by u^N and let the stabilisation parameters be chosen according to

$$\delta_{11} \leq C N^{-2} \left(\max |\psi'| \right)^{2p}, \tag{9a}$$
$$\delta_{21} \leq C \varepsilon^{-1/2} \ln^{-1} N \left(N^{-1} \max |\psi'| \right)^2, \tag{9b}$$
$$\delta_{12} = \delta_{22} = 0. \tag{9c}$$

Then, we have

$$\left| \left| \left| u - u^N \right| \right| \right|_\varepsilon \leq C C_\psi \left(N^{-1} \max |\psi'| \right)^p \tag{10}$$

and

$$\left| \left| \left| I^N u - u^N \right| \right| \right|_{LPS} \leq C C_\psi \left(N^{-1} \max |\psi'| \right)^p. \tag{11}$$

Proof. The first result (10) follows from the triangle inequality, (4) and (11).

In order to prove (11), we use coercivity and the weak Galerkin orthogonality of the stabilised method and obtain

$$\left| \left| \left| I^N u - u^N \right| \right| \right|_{LPS}^2 \leq a_{Gal} \left(I^N u - u, \chi \right) + s \left(I^N u, \chi \right).$$

Now the decomposition of Assumption 1 and anisotropic error estimates of I^N and κ_τ can be applied in the various subdomains of Ω.

For a complete proof see [12].

Note that in order to prove convergence of the LPSFEM no additional orthogonality of the interpolation operator is required and that the last estimate is a supercloseness result.

Remark 6. The factor C_ψ defined in (8) is bounded by a constant for Shishkin and the Bakhvalov-Shishkin meshes.

Remark 7. The choice (9) gives us the largest upper bounds for the whole class of S-type meshes such that convergence of order p holds. In particular, for the standard Shishkin mesh we obtain

$$\delta_{11} \le CN^{-2}\big(\ln N\big)^{2p}, \quad \delta_{21} \le C\varepsilon^{-1/2}N^{-2}\ln N, \quad \delta_{12} = \delta_{22} = 0 \tag{12}$$

while we get

$$\delta_{11} \le CN^{-2}, \quad \delta_{21} \le C\varepsilon^{-1/2}\ln^{-1} NN^{-2}, \quad \delta_{12} = \delta_{22} = 0. \tag{13}$$

for the Bakhvalov-Shishkin mesh.

5 Numerical Results

We consider the following singularly perturbed convection-diffusion problem for our numerical study:

$$-\varepsilon\Delta u - (2-x)u_x + \frac{3}{2}u = f \quad \text{in } \Omega \quad \text{and} \quad u = 0 \quad \text{on } \partial\Omega,$$

where the right-hand side f is chosen such that

$$u(x,y) = \left(\cos\frac{\pi x}{2} - \frac{\mathrm{e}^{-x/\varepsilon} - \mathrm{e}^{-1/\varepsilon}}{1-\mathrm{e}^{-1/\varepsilon}}\right)\frac{\left(1-\mathrm{e}^{-y/\sqrt{\varepsilon}}\right)\left(1-\mathrm{e}^{-(1-y)/\sqrt{\varepsilon}}\right)}{1-\mathrm{e}^{-1/\sqrt{\varepsilon}}}$$

is the solution. Note that Assumption 1 is satisfied.

The presented numerical results were obtained by the finite element package MooNMD [13]. All occurring systems of linear equations were solved directly by using package UMFPACK [6–9].

As parameters we use $\varepsilon = 10^{-12}$, $p = 5$, $\sigma = 6$. All numerical quadratures are carried out using a 8×8-Gaussian quadrature rule. For the LPSFEM we set the stabilisation parameters according to (12) for the Shishkin mesh and to (13) for the Bakhvalov-Shishkin mesh, both with $C = 0.001$.

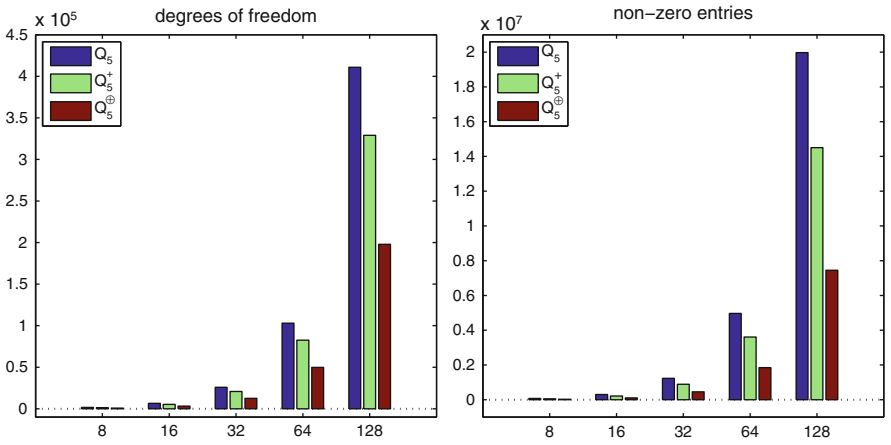

Fig. 3 Number of degrees of freedom (*left*), number of non-zero entries of stiffness matrix (*right*)

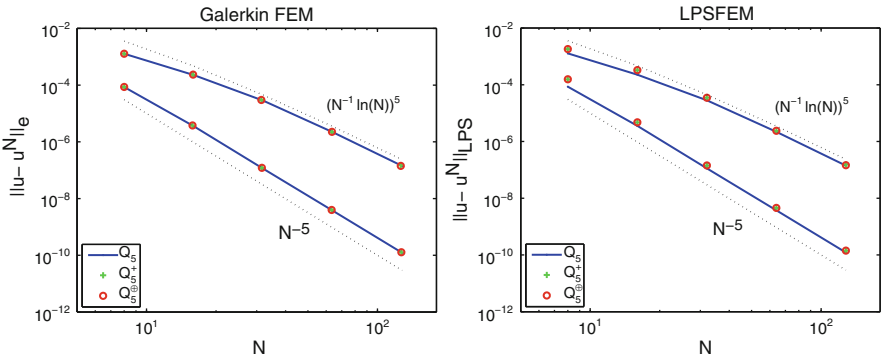

Fig. 4 Energy-norm errors for Galerkin FEM (*left*) and LPSFEM (*right*)

Figure 3 shows for three different choices of $\mathcal{Q}_p^{\clubsuit}$ the computational costs in terms of degrees of freedom and number of non-zero entries in the stiffness matrix. Clearly, the choice of the serendipity element $\mathcal{Q}_p^{\oplus}$ reduces the costs by a factor of about 2 compared to the full $\mathcal{Q}_p$-element while the standard enriched element $\mathcal{Q}_p^{+}$ [12], gained by taking $\widetilde{\mathcal{Q}}_p = \mathcal{Q}_{p-3} \oplus \operatorname{span}\{\xi^{p-2}, \eta^{p-2}\}$, lies in between.

Figure 4 shows the convergence of the two methods for the three different spaces on the Shishkin and the Bakhvalov-Shishkin mesh. The upper curves correspond to the Shishkin mesh and a convergence rate of $\mathcal{O}\left((N^{-1} \ln N)^5\right)$ is observable for the Galerkin FEM on the left and for the LPSFEM on the right. Note that the choice of the space has almost no effect on the quality of the computed solutions. However, the choice of the mesh has a much stronger effect – the lower curves correspond to the Bakhvalov-Shishkin mesh. We observe a convergence order of $\mathcal{O}\left(N^{-5}\right)$ and on the finest mesh three orders of magnitude difference.

Table 1 Galerkin discretisation with $Q_5^{\oplus}$, $N = 64$, and $\varepsilon = 10^{-12}$ for different point distribution types

	$\|u - u^N\|_\varepsilon$		$\|J^N u - u\|_\varepsilon$		$\|J^N u - u^N\|_\varepsilon$	
Type	S-mesh	B–S mesh	S-mesh	B–S mesh	S-mesh	B–S mesh
1	1.991-06	3.751-09	2.634-06	4.788-09	1.722-06	2.987-09
2	1.991-06	3.751-09	2.464-06	4.649-09	1.465-06	2.760-09
3	1.991-06	3.751-09	3.748-06	7.097-09	3.176-06	6.028-09

Table 2 Local projection stabilisation with $Q_5^{\oplus}$, $N = 64$, and $\varepsilon = 10^{-12}$ for different point distribution types

	$\|u - u^N\|_{LPS}$		$\|J^N u - u\|_{LPS}$		$\|J^N u - u^N\|_{LPS}$	
Type	S-mesh	B–S mesh	S-mesh	B–S mesh	S-mesh	B–S mesh
1	2.383-06	4.546-09	2.636-06	4.790-09	2.169-06	3.953-09
2	2.383-06	4.546-09	2.464-06	4.650-09	1.941-06	3.767-09
3	2.383-06	4.546-09	3.749-06	7.098-09	3.603-06	6.552-09

Finally, we want to study the influence of the distribution of the points which are used to define the interpolation operator $\mathcal{J}$. We have considered the case $\xi = \eta$ with three different choices:

type 1 equidistant point distribution $(-1, -0.6, -0.2, 0.2, 0.6, 1)$,

type 2 Gauss–Lobatto points $(-1, -0.765, -0.285, 0.285, 0.765, 1)$,

type 3 points condensed near 0 $(-1, -0.25, -0.083, 0.083, 0.25, 1)$.

Tables 1 and 2 show the errors for the methods based on the above given point distribution for a fixed mesh of $N = 64$. Clearly, the difference of the errors between those three different types is very small. Nevertheless, it can be observed that the Gauss-Lobatto points give the smallest interpolation- and closeness errors while type 3 generates the biggest errors. This is caused by the concentration of points near 0 which leads to a worse behaviour of the interpolation operator.

Since the finite element space V^N is not influenced by the choice of the interpolation points, the error $u - u^N$ is the same for all interpolation operators. This can be seen from the columns 2 and 3 in Tables 1 and 2.

Above consideration of the influence of point distributions on the behaviour of the interpolation operator J^N shows that it is sufficient to use an equidistant point distribution although the more sophisticated choice of Gauss–Lobatto points generates smaller interpolation errors.

Acknowledgements The author has been supported by Science Foundation Ireland under the Research Frontiers Programme 2008; Grant 08/RFP/MTH1536.

References

1. T. Apel. *Anisotropic finite elements: local estimates and applications*. Advances in Numerical Mathematics. B. G. Teubner, Stuttgart, 1999.
2. N. S. Bakhvalov. The optimization of methods of solving boundary value problems with a boundary layer. *U.S.S.R. Comput. Math. Math. Phys.*, 9(4):139–166, 1969.

3. R. Becker and M. Braack. A finite element pressure gradient stabilization for the Stokes equations based on local projections. *Calcolo*, 38(4):173–199, 2001.
4. R. Becker and M. Braack. A two-level stabilization scheme for the Navier-Stokes equations. In M. Feistauer, V. Dolejší, P. Knobloch, and K. Najzar, editors, *Numerical mathematics and advanced applications*, pages 123–130, Berlin, 2004. Springer-Verlag.
5. M. Braack and E. Burman. Local projection stabilization for the Oseen problem and its interpretation as a variational multiscale method. *SIAM J. Numer. Anal.*, 43(6):2544–2566, 2006.
6. T. A. Davis. Algorithm 832: UMFPACK V4.3—an unsymmetric-pattern multifrontal method. *ACM Trans. Math. Software*, 30(2):196–199, 2004.
7. T. A. Davis. A column pre-ordering strategy for the unsymmetric-pattern multifrontal method. *ACM Trans. Math. Software*, 30(2):167–195, 2004.
8. T. A. Davis and I. S. Duff. An unsymmetric-pattern multifrontal method for sparse LU factorization. *SIAM J. Matrix Anal. Appl.*, 18(1):140–158, 1997.
9. T. A. Davis and I. S. Duff. A combined unifrontal/multifrontal method for unsymmetric sparse matrices. *ACM Trans. Math. Software*, 25(1):1–20, 1999.
10. S. Franz. *Singularly perturbed problems with characteristic layers: Supercloseness and postprocessing*. PhD thesis, Department of Mathematics, TU Dresden, 2008.
11. S. Franz and G. Matthies. Convergence on Layer-Adapted Meshes and Anisotropic Interpolation Error Estimates of Non-Standard Higher Order Finite Elements. Mathematische Schriften Kassel 01/10, Universität Kassel, 2010. submitted for publication.
12. S. Franz and G. Matthies. Local projection stabilisation on S-type meshes for convection-diffusion problems with characteristic layers. *Computing*, 87(3–4):135–167, 2010.
13. V. John and G. Matthies. MooNMD - a program package based on mapped finite element methods. *Comput. Vis. Sci.*, 6(2–3):163–170, 2004.
14. R. B. Kellogg and M. Stynes. Sharpened and corrected version of: Corner singularities and boundary layers in a simple convection-diffusion problem. *J. Differential Equations*, 213(1):81–120, 2005.
15. T. Linß and M. Stynes. Numerical methods on Shishkin meshes for linear convection-diffusion problems. *Comput. Methods Appl. Mech. Eng.*, 190(28):3527–3542, 2001.
16. Linß, T. An upwind difference scheme on a novel Shishkin-type mesh for a linear convection-diffusion problem. *J. Comput. Appl. Math.*, 110(1):93–104, 1999.
17. G. Matthies, P. Skrzypacz, and L. Tobiska. A unified convergence analysis for local projection stabilisations applied to the Oseen problem. *M2AN Math. Model. Numer. Anal.*, 41(4):713–742, 2007.
18. J. J. H. Miller, E. O'Riordan, and G. I. Shishkin. *Fitted numerical methods for singular perturbation problems: Error estimates in the maximum norm for linear problems in one and two dimensions*. World Scientific Publishing Co. Inc., River Edge, NJ, 1996.
19. H.-G. Roos and T. Linß. Sufficient conditions for uniform convergence on layer-adapted grids. *Computing*, 63(1):27–45, 1999.
20. M. Stynes and E. O'Riordan. A uniformly convergent Galerkin method on a Shishkin mesh for a convection-diffusion problem. *J. Math. Anal. Appl.*, 214(1):36–54, 1997.
21. P. Sun, L. Chen, and J. Xu. Numerical studies of adaptive finite element methods for two dimensional convection-dominated problems. *J. Sci. Comput.*, 43:24–43, 2010.